



Research Article

Performance Evaluation of Clarithromycin as Aluminum Corrosion Inhibitor in H₂SO₄ Media

Ochili F. O., Onukwuli O. D. and Nnanwube I. A

Special Issue

A Themed Issue in Honour of Professor Onukwuli Okechukwu Dominic (FAS).

This special issue is dedicated to Professor Onukwuli Okechukwu Dominic (FAS), marking his retirement and celebrating a remarkable career. His legacy of exemplary scholarship, mentorship, and commitment to advancing knowledge is commemorated in this collection of works.

Edited by
Chinonso Hubert Achebe PhD.
Christian Emeka Okafor PhD.

Performance Evaluation of Clarithromycin as Aluminum Corrosion Inhibitor in H₂SO₄ Media

Ochili F. O¹., Onukwuli O. D.¹ and Nnanwube I. A.^{2*}

¹Chemical Engineering Department, Faculty of Engineering & Technology, Nnamdi Azikiwe University, P.M.B. 5025, Awka, Anambra State, Nigeria

²Chemical Engineering Department, Faculty of Engineering & Technology, Madonna University, Akpugo Campus, Enugu State, Nigeria

*Corresponding Author's E-mail: ik.nnanwube@gmail.com

Abstract

The potency of expired clarithromycin (CM) as an inhibitor for controlling aluminum (Al) corrosion in 1 M H₂SO₄ was studied using weight loss, impedance spectroscopy, and polarization measurements as experimental methods, and density functional theory (DFT) as theoretical method. The relevant groups in the inhibitor were identified with infrared spectroscopy. The heteroatoms detected by the infrared spectroscopy analysis showed the inhibitor's potency in checkmating aluminum corrosion in H₂SO₄ media. Further analysis of the inhibitor via gas chromatography-mass spectrometry specifies that bis(2-ethylhexyl) phthalate, cis-13-octadecenoic acid, cis-vaccenic acid, and others were contained in the inhibitor. The inhibitive power of clarithromycin rose with an increase in the inhibitor concentration (IC) and a reduction in temperature. The heat of adsorption (Q_{ads}) results at various inhibitor concentrations were all negative with a value of -60153.3 J/mol at clarithromycin concentration of 0.7 g/L. Maximum efficiency of 91.36% was attained from the gravimetric method. The impedance diagrams obtained showed depressed semicircles with various inhibitor concentrations. PDP analysis results showed the inhibitor as mixed-type. The DFT results showed further parameters that established clarithromycin as a suitable inhibitor. Adsorption studies indicated that the Langmuir model provided the best fitting to the results obtained from the experiment since it gave the highest average R² value. Gibb's free energy of adsorption values of -10.16 kJ/mol and -10.14 kJ/mol were recorded at 313 K and 323 K, respectively, indicating a physisorption process. An inhibition efficiency (IE) of 96.9 % was recorded with the EIS technique. Hence, clarithromycin was confirmed to be a suitable inhibitor for checkmating Al corrosion.

Keywords: Clarithromycin, H₂SO₄, Corrosion inhibitor, DFT, Aluminum

1. Introduction

Metal deterioration due to its interaction with aqueous corrosive environments (moisture, soil or air) through electrochemical or straight chemical reactions to give rise to noble compounds leads to a phenomenon known as corrosion. It is an interfacial material (ceramic, concrete, polymer, wood and metal) irreversible reaction with its surroundings which leads to material depletion or dissolution into the material of an environmental component. Corrosion poses an environmental menace with economic, maintenance and safety effects in numerous engineering areas such as automobile, building construction, mechatronics, medical, metallurgical, and chemical, amongst others (Ezeamaku et al., 2023; Onukwuli et al., 2021).

Corrosion inhibitors reduce or prevent corrosion when introduced in small concentrations to a corrosive medium by developing a unimolecular film-adsorbed surface which hinders direct interaction between corrosive agents and metal. Based on sources, inhibitors have been categorized (as inorganic or organic) and based on techniques (as extracted or

synthesized). Hence, there is a need to source for not only appropriate corrosion inhibitors but environmentally friendly and economically viable ones. Several techniques, electrochemical and chemical methods have been utilized to examine metal corrosion in several hostile media. The utilization of inhibitors is among the proven means of protecting metal surfaces from dissolution (Anadebe et al., 2019; Emereole et al., 2024).

Acid media (such as HCl and H₂SO₄ solutions) used for the pickling of metallic structures have the side effect of corroding the metals. Hence, corrosion inhibitors are needed in the preparation of pickling solutions. Many works have been conducted on artificial materials as corrosion inhibitors, but the majority of them are very costly and not environment-friendly. Currently, the emphasis is on the deployment of polymeric materials, ionic liquids, plant extracts and pharmaceutical drugs. Drugs are of great interest because they are already developed recipes and expired drugs are readily available. Oftentimes, the drugs expire as a result of a low record of sales. Diversification of their usage will encourage high demand for the drugs in industrial applications (Udunwa et al., 2024; Omotioma et al., 2024).

Clarithromycin (CM) is a drug that prevents protein synthesis. It specifically binds to a 50S ribosomal subunit, which inhibits the peptidyl chain's elongation cycle. They are applied to address a wide range of skin-related bacterial diseases. In our previous publication (Onukwuli et al. (2025)), the effectiveness of CM as an inhibitor for Al in HCl media was reported. The present study seeks to probe further by examining the inhibitive effect of clarithromycin in 1 M H₂SO₄ media with various methods such as weight loss, potentiodynamic polarization (PDP), electrochemical impedance spectrometry (EIS), and density functional theory computations.

2.0 Materials and methods

2.1 Concentrated gestid preparation

Various concentrations of the expired drug were prepared. In each flask containing one liter of H₂SO₄ solution, ten (10) grams of clarithromycin was added. Inhibitor test solutions were prepared at 0.1 - 0.9 g/L concentrations from the 10 g/L stock (Onukwuli et al., 2024(a, b); Dheenadhayalan et al., 2018).

2.2 Preparation of metals

Aluminum coupons used were made of V (0.04%), Si (0.25%), Fe (0.02%), Ti (0.12%), Zn (0.07%), Mg (0.03%), Mn (0.14%), Al (99.3%), Cu (0.03%). The detailed procedure of the metal preparation had earlier been described (Onukwuli et al., 2024 (a, b)).

2.3 Characterization of the inhibitor

With the aid of a GC-MS, a chemical examination of clarithromycin was performed. When heated in the GC, the drug disintegrated into separate substances. They were then passed through an inert gas column filled with nitrogen. When the isolated substances appeared from the opening in the column, they hovered into the MS where the compounds in the inhibitor were made known using the analyte molecule's mass. Cary 630 model FTIR spectroscopy from Agilent Technologies was applied to examine the inhibitor's functional groups as earlier reported (Onukwuli et al., 2024 (a, b); Singh et al., 2015).

2.4 Inhibition Process Thermometry

This comprises the determination of inhibition efficiency (IE) and reaction number (RN). Equation (1) was utilized to calculate the RN while Eq. (2) was deployed in computing the IE (Onukwuli et al., 2025; Elkatatny et al., 2024).

$$RN = \frac{T_m - T_i}{t} \quad (1)$$

$$IE(\%) = \left(1 - \frac{RN_{inh}}{RN_{uninh}}\right) * 100 \quad (2)$$

2.5 Weight loss technique

The weight loss (Δw) method was deployed as earlier described. The Δw , corrosion rate (CR), and IE, respectively, were estimated by applying Eqs. (3), (4), and (5). Equation (6) was deployed to compute the surface coverage (θ) as reported by Haque et al. (2023), Onukwuli et al. (2025) and Wan Nik et al. (2023).

$$\Delta w = w_i - w_f \quad (3)$$

$$CR = \frac{w_i - w_f}{At} \quad (4)$$

$$IE \% = \frac{\omega_0 - \omega_1}{\omega_0} \times 100 \quad (5)$$

$$\theta = \frac{\omega_0 - \omega_1}{\omega_0} \quad (6)$$

2.6 Estimation of the activation energy (E_a) and heat of adsorption (Q_{ads})

Equations (7) – (9) were employed to compute the E_a and Q_{ads} as reported in previous works (Emereole et al., 2024; Omotioma et al., 2024; Onukwuli et al., 2024 (a, b)).

$$\ln(CR) = \ln A - \left(\frac{E_a}{R}\right) \frac{1}{T} \quad (7)$$

$$\ln\left(\frac{CR_2}{CR_1}\right) = \ln A - \left(\frac{E_a}{2.303R}\right) \left(\frac{1}{T_1} - \frac{1}{T_2}\right) \quad (8)$$

$$Q_{ads} = 2.303R \left[\log \frac{\theta_2}{1-\theta_2} - \log \frac{\theta_1}{1-\theta_1} \right] * \frac{T_2 \cdot T_1}{T_2 - T_1} \quad (9)$$

2.6.1 Adsorption models

The surface coverage (θ) results were utilized to examine the usefulness of various isotherm models, comprising the Frumkin, Langmuir, Temkin, and Flory-Huggins model as respectively given in Eqs. (10) – (13) as applied by Onukwuli et al. (2024 (a, b), 2025), Udunwa et al. (2023), and Popoola et al. (2023).

$$\log \left[\left(C \times \left(\frac{\theta}{1-\theta} \right) \right) \right] = 2.303 \log K + 2\alpha\theta \quad (10)$$

$$\frac{C}{\theta} = \frac{1}{K_{ads}} + C \quad (11)$$

$$\theta = -\frac{2.303 \log K}{2\alpha} - \frac{2.303 \log C}{2\alpha} \quad (12)$$

$$\log \left[\left(\frac{\theta}{C} \right) \right] = \log K + x \log (1-\theta) \quad (13)$$

where x , α , θ , K , and C respectively signify the size parameter, lateral interaction term, surface coverage, equilibrium constant, and inhibitor (clarithromycin) concentration. The adsorption free energy (ΔG_{abs}) was estimated using Eq. (14).

$$\Delta G_{abs} = -2.303RT \log (55.5K) \quad (14)$$

2.7 Analysis of Electrochemical Techniques

A previously reported technique was applied in analyzing the PDP and EIS measurements. Measurements were performed in an unstretched and aerated solution after 1800 seconds of immersion, allowing the open circuit potential to reach a steady state. 30 ± 1 °C was maintained as the temperature of the system (Onukwuli et al., 2025; Farag et al., 2015).

2.8 DFT computation and modeling

DFT computation and modeling were deployed to define the adhesive characteristics of the molecular composition of clarithromycin as previously reported (Onukwuli et al., 2025).

3. Results and discussions

3.1 Infrared spectroscopy results of clarithromycin

The relevant functional groups of clarithromycin obtained by FTIR are C-N, C=C, O-H, C-Cl, C=O, C=N stretches, C-O-C, C-H, SO₂ stretches (anti-symmetrical), and others. The heteroatoms found in the drug suggest that it is fit for inhibiting corrosion (Onukwuli et al., 2025).

3.2 Thermometry results

Table 1 illustrates the effects of CM concentrations on the RN and IE. The CM concentration range used was 0.1 - 0.9 g/L. The reaction number reduced with a rise in the CM concentration till CM concentration of 0.7 g/L, after which it increased. This is in agreement with the reports of Omotioma et al. (2024) and Udeh et al. (2021). In general, IE increased while the RN decreased as the IC was increased.

Table 1: Effect of the concentration of the inhibitor on the RN and IE of aluminum in H₂SO₄ media

Inhibitor conc. (g/L)	0.0	0.1	0.3	0.5	0.7	0.9
RN (°C/min)	0.3154	0.0836	0.0648	0.0373	0.0324	0.0398
IE (%)		73.49	79.46	88.19	89.74	87.4

3.3 Weight loss results

Table 2 presents the influence of control factors such as temperature, concentration, and time for checkmating aluminum corrosion in H₂SO₄. In the uninhibited medium, corrosion rate (CR₀) and weight loss (ΔW₀) were higher compared to CR₁ and ΔW₁ of the clarithromycin-H₂SO₄ media. The results obtained show a reduction in ΔW and CR and consequently, an increase in the IE as the IC increased. As displayed in Table 2, IE from this study increased from 81.33 % obtained in 4 hours to 83.02 % in 3 hours at 303 K and 91.36% in 5 hours at 303 K, indicating no linearity in the correlation between time and IE. An increase in clarithromycin concentration led to the increase in IE as recorded in Table 2. The effectiveness of the inhibition process was achieved by decreasing the passivation oxide film's dissolution rate as well as its repair (Ezeamaku et al., 2023; Onyenanu et al., 2023). The maximum inhibition efficiency recorded here (91.36 %) is higher than the value of 87.36 % obtained when clarithromycin was applied as inhibitor for aluminum corrosion in HCl media at a temperature of 303 K and CM concentration of 0.9 g/L (Onukwuli et al. (2025)). The maximum IE obtained from this work is also higher than the maximum value obtained when danacid was used as an inhibitor for checkmating aluminum corrosion in H₂SO₄ (88.10 %) (Onukwuli et al., 2024a) and HCl (78.35 %) (Onukwuli et al., 2024b) media at the same experimental conditions.

3.4 Estimation of the E_a and Q_{ads}

The E_a and Q_{ads} results for curbing aluminum corrosion in H₂SO₄ with CM are presented in Tables 3 and 4. The Arrhenius equation was utilized to estimate the activation energy. This equation displays the relationship between the CR and the reciprocal of temperature (absolute). The E_a recorded from this study suggests that the inhibition process followed physical adsorption. This shows that clarithromycin is fitting for impeding Al corrosion. Q_{ad} is a significant parameter since it shows a direct connection with θ. Q_{ads} obtained are all negative as shown in Table 4, signifying an exothermic adsorption process of the inhibitor (Onukwuli et al., 2024 (a, b)).

Table 2: Weight loss, CR, IE and SC of aluminum in sulphuric acid with clarithromycin as an inhibitor

Time (h)	Temp (K)	Inhibitor conc. (g/L)	(IC)	wt loss, Δw (g)	Corrosion rate, CR (g/cm ² h)	Inhibition efficiency, IE (%)	Surface coverage, SC (θ)
5	303	0.0		0.081	0.0018		
		0.3		0.036	0.0008	55.56	0.5556
		0.7		0.022	0.0005	72.84	0.7284
		0.9		0.007	0.0002	91.36	0.9136
	313	0.0		0.093	0.0021		
		0.3		0.045	0.001	51.61	0.5161
		0.7		0.028	0.0006	69.89	0.6989
		0.9		0.021	0.0005	77.42	0.7742
	323	0.0		0.113	0.0025		
		0.3		0.055	0.0012	51.33	0.5133
		0.7		0.037	0.0008	67.26	0.6726
		0.9		0.031	0.0007	72.57	0.7257
4	303	0.0		0.075	0.0021		
		0.3		0.035	0.0010	53.33	0.5333
		0.7		0.022	0.0006	70.67	0.7067
		0.9		0.014	0.0004	81.33	0.8133
	313	0.0		0.084	0.0023		
		0.3		0.042	0.0012	50.00	0.5000
		0.7		0.027	0.0008	67.86	0.6786
		0.9		0.021	0.0006	75.00	0.7500
	323	0.0		0.098	0.0027		
		0.3		0.051	0.0014	47.96	0.4796
		0.7		0.040	0.0011	59.18	0.5918
		0.9		0.032	0.0009	67.35	0.6735
3	303	0.0		0.053	0.0020		
		0.3		0.027	0.0010	49.06	0.4906
		0.7		0.020	0.0007	62.26	0.6226
		0.9		0.009	0.0003	83.02	0.8302
	313	0.0		0.064	0.0024		
		0.3		0.035	0.0013	45.31	0.4531
		0.7		0.025	0.0009	60.94	0.6094
		0.9		0.019	0.0007	70.31	0.7031
	323	0.0		0.069	0.0026		
		0.3		0.039	0.0014	43.48	0.4348
		0.7		0.030	0.0011	56.52	0.5652
		0.9		0.022	0.0008	68.12	0.6812

Table 3: E_a for controlling Al corrosion in H₂SO₄

Temperature (K)	303	313	323	333	343
E_a (kJ/mol)	23.16				
CR (mg/cm ² h)	1.139	0.917	1.722	2.333	2.75

Table 4: Q_{ads} values estimated

Inhibitor conc. (g/L)	0.1	0.3	0.5	0.7	0.9
Q_{ads} (J/mol)	-32578.6	-45971.6	-64584.3	-60153.3	-51567.4

3.5 Adsorption parameters

Parameters of the Temkin, Langmuir, Frumkin and Flory-Huggins isotherms for checkmating aluminum corrosion in H_2SO_4 media are shown in Table 5. The results obtained show that Langmuir isotherm is the model that best fits the results obtained. This assertion was based on the maximum recorded average value of R^2 which was closest to the critical value of 1 (one) compared to the R^2 values of other isotherms (Temkin, Flory-Huggins and Frumkin). The attractive parameter (a) values obtained from the Temkin plots are negative indicating that no chemical reaction occurred between aluminum and clarithromycin. The lateral interaction term (α) at 313 K and 323 K are positive, suggesting that there was a noticeable attraction between clarithromycin and aluminum surface. The positive size property (x) values obtained from the Flory-Huggins isotherm indicated a reasonable layer of drug attachment to the aluminum surface. The Gibb's free energy (ΔG_{ads}) obtained is lower than -40.00 kJ/mol, inferring a physisorption process. The negative value of ΔG_{ads} designates a spontaneous process of adsorption (Onukwuli et al., 2024 (a, b)). The isotherm plots are shown in Figures (1-4).

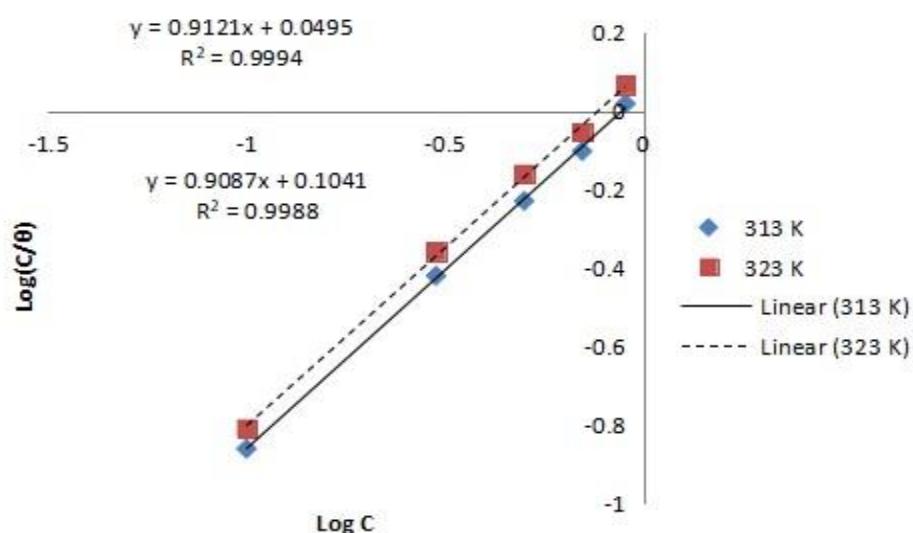


Figure 1: Plots of Langmuir model

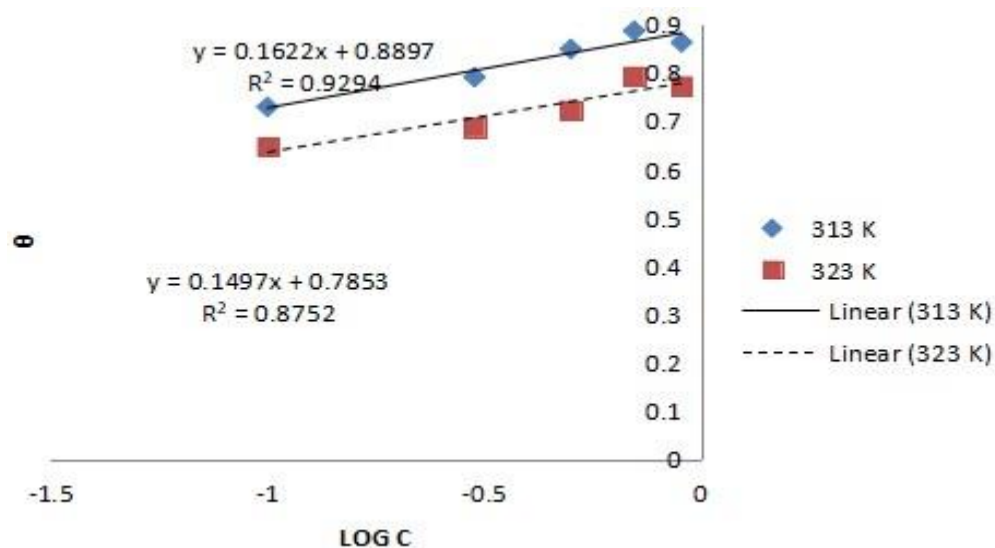


Fig. 2: Plots of Temkin model

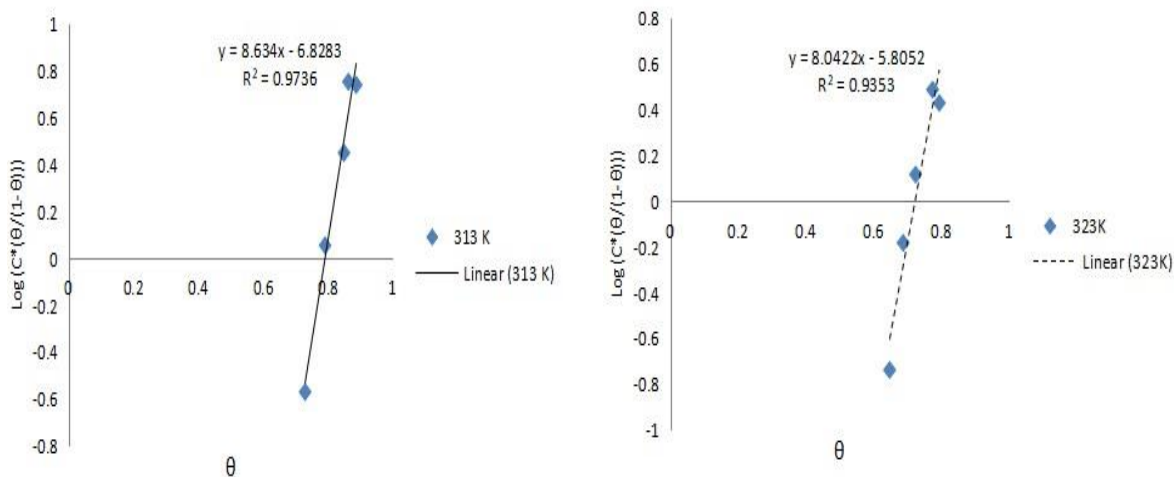


Figure 3: Plots of Frumkin model

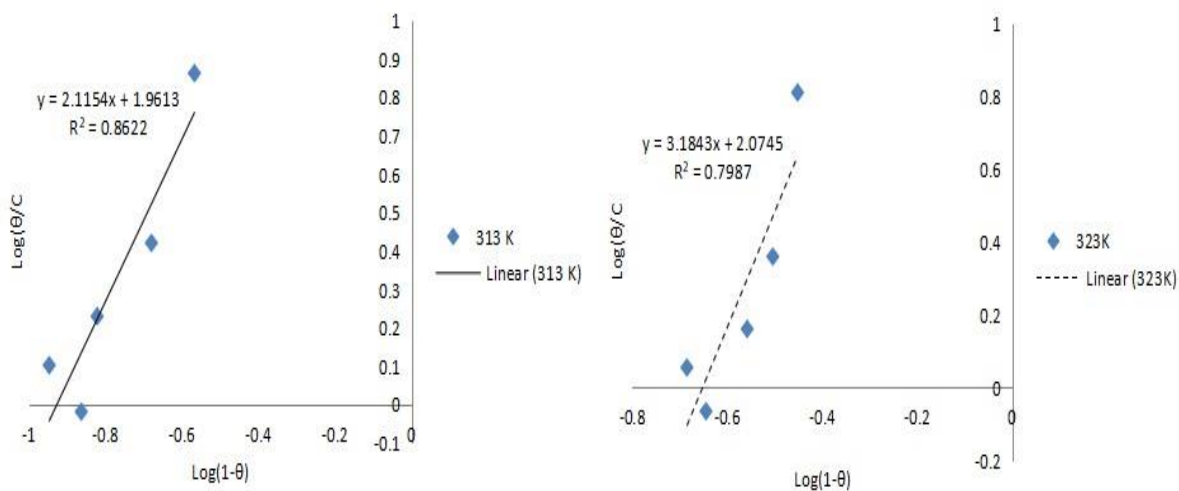


Figure 4: Plots of Flory-Huggins model

Table 5: Parameters of adsorption models for controlling Al corrosion in H₂SO₄

Isotherm model	Temp. (K)	R ²	K	ΔG _{ads} (J/mol)	Property of isotherm
Langmuir Isotherm	313	0.9994	0.8923	-10157.0536	
Langmuir Isotherm	323	0.9988	0.7868	-10143.5971	
Temkin Isotherm	313	0.9294	9 × 10 ¹⁰	-76103.0273	a -14.1985
Temkin Isotherm	323	0.8752	3.10 × 10 ¹⁰	-75671.7351	-15.3841
Frumkin Isotherm	313	0.9736	0.0011	7277.45311	α 4.317
Frumkin Isotherm	323	0.9353	0.0030	4815.1846	4.0211
Flory-Huggins Isotherm	313	0.8622	91.4745	-22207.8245	x 2.1154
Flory-Huggins Isotherm	323	0.7987	118.7135	-23617.4285	3.1843

3.6 PDP results

Figure 5 portrays the plots of aluminum samples in the clarithromycin-H₂SO₄ and free media from the PDP analysis. In the range of measurement, the Al sample in the H₂SO₄ solution demonstrated high dissolution devoid of any indication of passivation. The range of - 250 to + 2000 mV was used to perform the PDP test for aluminum. Throughout the study, a 0.5mV/s scan rate was maintained. A shift in both the anodic and cathodic sides of the plot specified that the inhibition is mixed-type, which agrees with previous reports (Hoseinpoor and Davoodi, 2015; Onukwuli et al, 2021). Table 6 portrays the PDP results for curbing Al corrosion in H₂SO₄ in the clarithromycin-H₂SO₄ and free solution. The corrosion current density (I_{corr}), corrosion potential (E_{corr}), and IE are displayed in Table 6. The results show that I_{corr} decreased in the clarithromycin-H₂SO₄ solution when compared with the free solution. This process increases as the inhibitor's active species concentration increases. The inhibition trend in Table 6 is ascribed to the harsh intermolecular connection between the valence electrons on the aluminum surface and the protonated CM molecules. From Table 6, it is obvious that a rise in the concentration of CM resulted in a reduction in the cathodic and anodic Tafel slopes (β_c and β_a), and corrosion potential (E_{corr}) increases signifying the inhibiting effect of CM on the Al surface owing to blocking of mechanism of adsorption. This compound performed as a mixed-type inhibitor, largely cathodic, though the cathode is less polarized on the application of an external current density ($\beta_c < \beta_a$). Hence, the CM molecule adsorb on both cathodic and anodic sites on the Al surface, obstructing the metal and the corrosive medium. The I_{corr} decreases and the IE rises, signifying the inhibiting influence of CM on Al corrosion in 1 M H₂SO₄.

Hence, clarithromycin foiled cathodic and anodic metal dissolution. An inhibitor is typically categorized as cathodic or anodic if the difference in E_{corr} value on adding it is larger than 85 mV. When the difference is not up to 85 mV, the clarithromycin may be characterized as mixed-type (MT-I). Therefore, the results recorded in this study show that clarithromycin is M-TI. The IE recorded in this study conforms with the one obtained by EIS, indicating that CM can effectively curb Al corrosion. The IE was computed with Eq. (15) (Abdallah et al., 2016; Onukwuli et al., 2025; Anadebe et al., 2019; Ezeamaku et al., 2023).

$$IE(\%) = \frac{i_{corr}^0 - i_{corr}^i}{i_{corr}^0} \times 100 \quad (15)$$

where i_{corr}^0 and i_{corr}^i are respectively the current density in the free and CM-H₂SO₄ media.

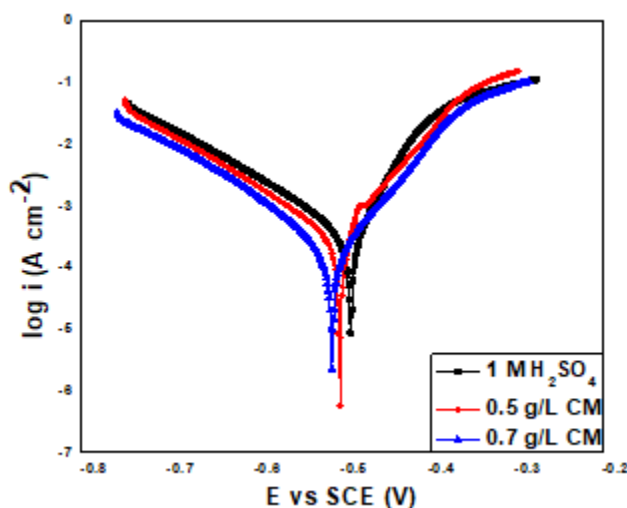


Figure 5: PDP graph for curbing Al corrosion in the free and inhibited media

Table 6: PDP measurement results

Media	E_{corr} (mV)	I_{corr} ($\mu\text{A}/\text{cm}^2$)	b_a (mVdec ⁻¹)	$-b_c$ (mVdec ⁻¹)	sc(0)	IE (%)
1 M H ₂ SO ₄	-448.5	178.4	89.5	45.7		
1 M H ₂ SO ₄ + 0.5g/L CM	-514.7	16.1	93.6	52.8	0.9098	90.98
1 M H ₂ SO ₄ + 0.7g/L CM	-421.5	12.8	87.4	40.3	0.9283	92.83

3.7. Electrochemical impedance spectroscopy (EIS)

Nyquist diagrams of Al in H₂SO₄ solution in the uninhibited and the CM-H₂SO₄ solutions are given in Fig. 6((a) Nyquist (b) Bode phase angle and (c) Bode modulus plots). As depicted in Fig. 6, the impedance diagrams display semi-circles signifying a barricade layer formed on the aluminum surface.

The IEs computed from the impedance tests are obtained by Eq. (16).

$$IE\% = [1 - (R_{ct}^o/R_{ct})] \times 100 \quad (16)$$

where R_{ct}^o and R_{ct} respectively designate charge transfer resistance in the uninhibited and inhibited medium. The impedance parameters, e.g. the inhibition efficiency (%IE), charge transfer resistance (R_{ct}), the capacitance double layer (C_{dl}), estimated from Nyquist plot curves are displayed in Table 7. The double-layer capacitance is computed from Eq. (17).

$$C_{dl} = 1/(2\pi f_{max} R_{ct}) \quad (17)$$

where f_{max} is the maximum frequency. Table 7 shows that the value of R_{ct} rises and the C_{dl} values reduce as the inhibitor concentration rises. This is credited to the gradual substitution of water molecules via the inhibitor molecules' adsorption to the surface of the metal, thereby reducing the degree of dissolution. Bigger values of R_{ct} are usually linked with the more sluggish corroding system. The reduction in the C_{dl} can occur from the reduction of the local dielectric constant signifying that the molecules of the inhibitor operate by adsorption at the solution/metal boundary (Abdallah et al., 2016; Onukwuli et al., 2024 (a, b)).

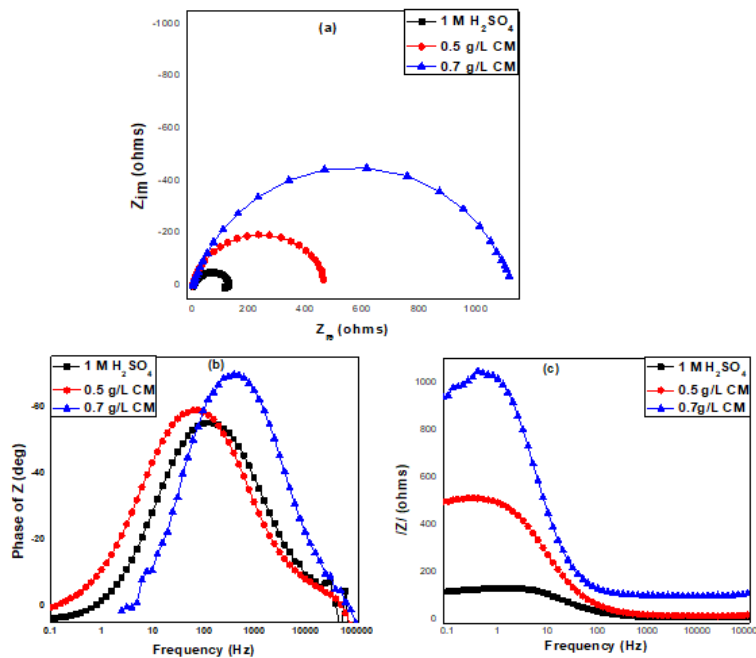


Figure 6: Impedance spectra of Al: Nyquist (a) Bode phase angle (b) and Bode modulus (c) plots in 1 M H₂SO₄ in the uninhibited and inhibited media

Table 7: EIS results of aluminum in H₂SO₄

Media	R _s (Ωcm ²)	R _{ct} (Ωcm ²)	N	C _{dl} (Fcm ²)	Inhibition efficiency (%)
1 M H ₂ SO ₄	1.625	32.4	0.89	7.084E-5	
1 M H ₂ SO ₄ + 0.5g/L CM	1.793	492.5	0.87	7.195E-5	93.42
1 M H ₂ SO ₄ + 0.7g/L CM	1.982	1043.5	0.86	7.174E-5	96.90

3.8. GC-MS Results

The GC-MS results of clarithromycin have been reported (Onukwuli et al., 2025). The components found include 1-Menthone, 2,4-Di-tert-butylphenol, Pentadecane, decyl hexadecyl ester, 1-Docosene, butyl octyl ester, 2-tetradecyl ester, 10-Heneicosene, 1,2-Benzenedicarboxylic acid, dodecyl ester, n-Hexadecanoic acid, Dibutyl phthalate, cis-13-Octadecenoic acid, cis-Vaccenic acid, Diisooctyl phthalate, 17-Pentatriacontene, trans-13-Octadecenoic acid, and others.

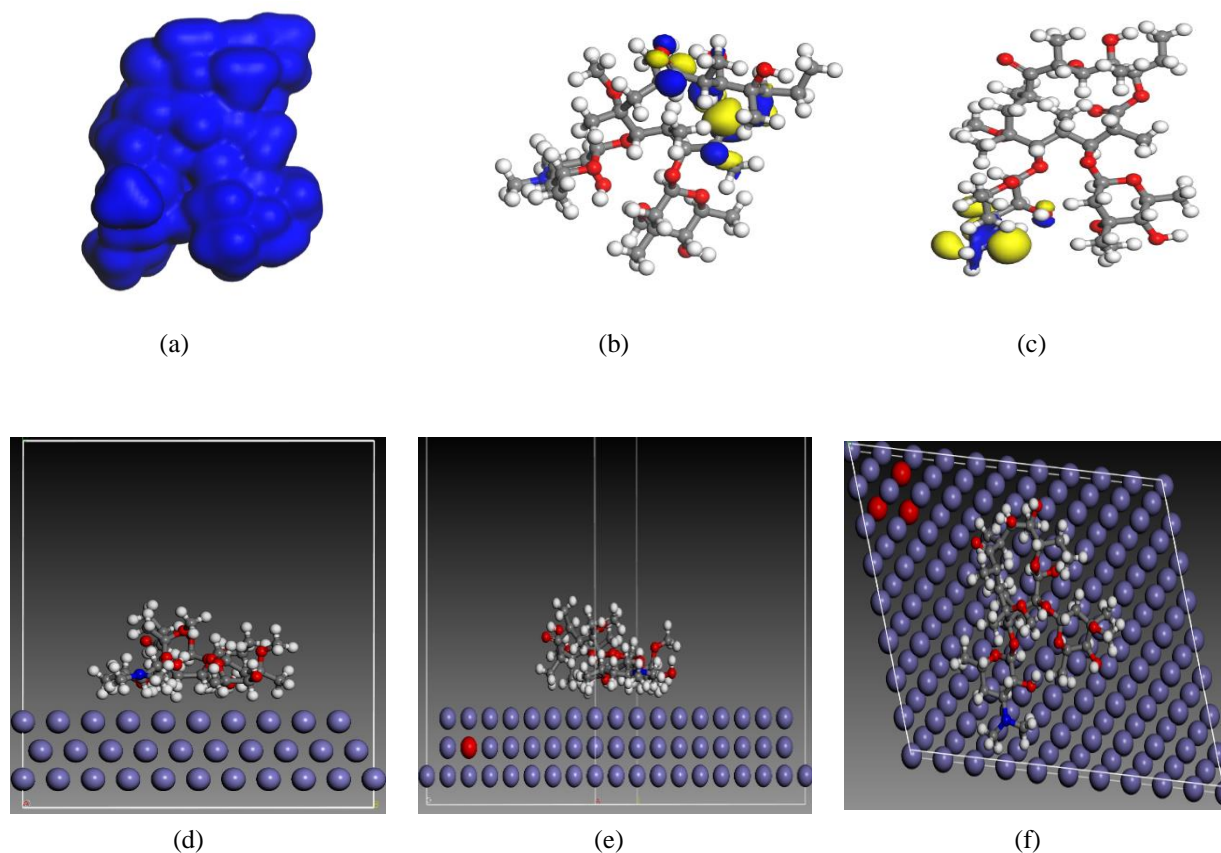


Figure 7: Clarithromycin, CM (C₃₈H₆₉NO₁₃): (a) Electron Density (b) LUMO (c) HOMO (d) Front View (e) Side View (f) Top View

3.9. DFT computation and modeling

DFT modeling was performed to give more explanation on the characteristics of molecules of clarithromycin as an inhibitor by assessing the structural properties of the compounds seen in it. Figure 7 (a-f) displays the various models of clarithromycin (C₃₈H₆₉NO₁₃) on the Al surface. Clarithromycin molecules fit into the notion that exceptional inhibitors, aside from donating electrons to the vacant orbital of the metal, also receive electrons available from the metal. From the postulation of frontier orbital theory, E_{HOMO} represents the aptitude of a species to contribute electrons,

signifying that the bigger the E_{HOMO} values the more likely it is to achieve outstanding efficiency of protection. Also, E_{LUMO} represents the aptitude of a species to receive electrons, hence, an excellent corrosion inhibitor is characterized by the low value of E_{LUMO} . The variance existing between the E_{LUMO} and E_{HOMO} depicts the energy gap (ΔE) of a molecule. Low ΔE value molecules may deliver better proficiency of protection. The results show that CM has high E_{HOMO} (-5.156 eV) and low E_{LUMO} (-3.418 eV) (Anadebe et al., 2019). The electrostatic interface between the charged molecule centers and charged metal surface which leads to a dipole contact of the metal surface and molecule gives rise to physical adsorption.

4. Conclusion

This work focused on the use of expired clarithromycin for controlling aluminum corrosion in 1 M H_2SO_4 medium using weight loss, electrochemical and theoretical techniques. The results of characterization studies portrayed excellent inhibitive properties for the inhibitor with the presence of heteroatoms as its constituents. The IE rose with the increase in CM concentration, up to 91.36 % at a concentration of 0.9 g/L; the IE, however, reduced with a rise in temperature. From the adsorption studies, it was found that expired clarithromycin followed Langmuir model with -10.2 kJ/mol Gibb's free energy at 313 K in a physisorption and spontaneous process. The polarization diagrams obtained showed that the inhibitor is mixed-type in 1 M H_2SO_4 , affecting both cathodic and anodic reactions. EIS measurements performed indicated that the IE of clarithromycin rose with the rise in charge transfer resistance and got to a value of 96.9%. Quantum chemical computations carried out indicate that the inhibitive power of expired clarithromycin was directly related to its HOMO and LUMO energies and tended to act as an electron-donor to the metal surface which could result to the development of an organic film capable of preventing corrosion on the aluminium surface in 1 M H_2SO_4 . The theoretical and experimental results indicated good consistency with each other. Hence, this study has further buttressed the viability of expired pharmaceuticals as inhibitors for checkmating corrosion in the industry. Further research may focus on the application of clarithromycin as an inhibitor for mild steel corrosion in different acidic and other corrosive media.

References

- Abdallah, M., Kamar, E. M., Eid, S., El-Etre, A. Y., 2016. Animal glue as green inhibitor for corrosion of aluminium and aluminium-silicon alloys in sodium hydroxide solutions. *Journal of Molecular Liquids* 220, 755-761. <http://dx.doi.org/10.1016/j.molliq.2016.04.062>
- Anadebe, V. C., Onukwuli, O. D., Omotioma, M., Okafor, N. A., 2019. Experimental, theoretical modeling and optimization of inhibition efficiency of pigeon pea leaf extract as anti-corrosion agent of mild steel in acid environment. *Materials Chemistry and Physics* 233, 120-132. <https://doi.org/10.1016/j.matchemphys.2019.05.033>
- Dheenadhayalan. S., Roja, R., Nijarubini, V., Mallika, J., 2018. Synergistic Effect Between Gum Exudates of Eucalyptus Globles and 2,6-Diphenyl-3-Methylpiperidin-4-one on Corrosion Inhibition of MS in 1N HCl. *Oriental Journal of Chemistry* 34(5) 2570-2576. <http://dx.doi.org/10.13005/ojc/340545>
- Ezeamaku, U. L., Eze, I., Odimegwu, N., Nwakaudu, A., Okafor, A., O. D. Onukwuli, O. D., Nnanwube, I. A., 2023. Corrosion inhibition of aluminium in 0.3 M HCl using starch mucor in potassium iodide as inhibitor. *Pigment & Resin Technology*, 53 (6) (2023)730-741. <https://doi.org/10.1108/PRT-12-2022-0152>.
- Elkatatny, S., Zaky, L., Abdelaziem, W., Abdelfatah, A., 2024. Optimizing corrosion resistance of $\text{Fe}_{35}\text{Ni}_{20}\text{Cr}_{12}\text{Mn}_{28}\text{Al}_5$ high-entropy alloy: synergistic effect of Mo inhibitor, Al content and cold rolling. *Anti-Corrosion Methods and Materials*, 71(4), 368-379. <https://doi.org/10.1108/ACMM-12-2023-2937>
- Emereole, J. C., Njoku, C. N., Ikeuba, A. I., Ekeke, I. C., Yakubu, E., Nkuzinna, O. C., Nnodum, N. A., M. S. Nwakaudu, M. S., 2024. Response surface methodology and experimental evaluation of the inhibitory

- properties of corn leaf extract for aluminum corrosion in acid media, [Anti-Corrosion Methods and Materials](#), 71 (6), 593-605. <https://doi.org/10.1108/ACMM-03-2024-2988>
- Frag, A. A., Ismail, A. S., Migahed, M. A., 2015. Inhibition of carbon steel corrosion in acidic solution using some newly polyester derivatives. *Journal of Molecular Liquids*, 211, 915-923. <https://doi.org/10.1016/j.molliq.2015.08.033>
- Haque, J., Zulaikha, M. A., Wan Nik, W. B., Daoudi, W., Berdimurodov, E., Zulkifli, F., 2023. Alocasia Odora Extract as Environmentally Benign Corrosion Inhibitor for Aluminum in HCl. *Mor. J. Chem.*, 11(4), 1013-1026. <https://doi.org/10.48317/IMIST.PRSM/morjchem-v11i04.41618>
- Hoseinpoor, M., Davoodi, A., 2015. Studies on corrosion-inhibiting performance of antithyroid drugs on mild steel in hydrochloric acid. *Research on Chemical Intermediates*, 41, 4255-4272. <https://doi.org/10.1007/s11164-013-1527-z>
- Omotioma, M., Onukwuli, O. D., Nnanwube, I. A., 2024. Testing the inhibition efficiency of the castor oil leaf as corrosion inhibitor of mild steel in H₂SO₄. *Heliyon*, 10, e31168. <https://doi.org/10.1016/j.heliyon.2024.e31168>
- Onukwuli, O. D., Nnanwube, I. A., Ochili, F. O., Omotioma, M., 2024a. DFT, Experimental and Optimization Studies on the Corrosion Inhibition of Aluminium in H₂SO₄ with Danacid as Inhibitor. *Results in Engineering*, 24, 103113. <https://doi.org/10.1016/j.rineng.2024.103113>
- Onukwuli, O. D., Nnanwube, I. A., Ochili, F. O., Obibuenyi, J. I., 2024b. Assessing the efficiency of danacid as corrosion inhibitor for aluminium in HCl medium: Experimental, theoretical and optimization studies, *Heliyon* 10, e40994. <https://doi.org/10.1016/j.heliyon.2024.e40994>
- Onukwuli, O. D., Nnanwube, I. A., Ochili, F. O., Omotioma, M., Obibuenyi, J. I., 2025. Corrosion inhibition effects of eco-friendly clarithromycin molecules on aluminium in hydrochloric acid solution via experimental, theoretical and optimization approach, *Results in Chemistry* 13, 101987. <https://doi.org/10.1016/j.rechem.2024.101987>
- Onukwuli, O. D., Udeh, B. C., Omotioma, M., Nnanwube, I. A., 2021. Corrosion Inhibition of Aluminium in Hydrochloric Acid Medium Using Cimetidine as Inhibitor: Empirical and Optimization Studies. *Anti-Corrosion Methods and Materials*, 68 (5), 385-395. <https://doi.org/10.1108/ACMM-03-2021-2447>.
- Onyenanu, C. N., Emembolu, L. N., Ejiofor, C. C., 2023. Corrosion Inhibition Potentials of A. mossambicensis and E. sonchifolia leaves' Extract on Aluminium in Alkaline Media: Insights from Gravimetric and Electrochemical Studies. *Chemistry Africa*, 6, 999-1014. <https://doi.org/10.1007/s42250-022-00531-0>
- Popoola, L. T., Yusuff, A. S., Ikumapayi, O. M., Chima, O. M., Ogunyemi, A. T., Obende, B. A., 2023. Carbon steel behavior towards Cucumeropsis mannii shell extract as an eco-friendly green corrosion inhibitor in chloride medium, *Scientific African* 21, e01860. <https://doi.org/10.1016/j.sciaf.2023.e01860>
- Singh, B., Khan, Z. A., Siddiquee, A. N. 2015. Effect of Minor Additives on Bead Geometry and Shape Relationship Using Submerged Arc Welding Fluxes. *Journal for Manufacturing Science and Production*, 15(2), 183-196. <https://doi.org/10.1515/jmsp-2014-0020>

- Udeh, B. C., Onukwuli, O. D., Omotioma, M., 2021. Corrosion Control of Aluminium in H₂SO₄ Medium Using Kolestran (Cholestyramine) Drug as Inhibitor. World Scientific News, 159, 95-107.
- Udunwa, D. I., Onukwuli, O. D., Menkiti, M. C., Anadebe, V. C., Chidiebere, M. A., 2023. 1-Butyl-3-methylimidazolium methane sulfonate ionic liquid corrosion inhibitor for mild steel alloy: Experimental, optimization and theoretical studies. Heliyon, 9(7), e18353. <https://doi.org/10.1016/j.heliyon.2023.e18353>
- Udunwa, D. I., Onukwuli, O. D., Menkiti, M. C., Nwanonenyi, S. C., Ezekannagha, C. B., Aniagor, C. O., 2024. Experimental, computational, and theoretical studies on the corrosion inhibition potential of green Gongronema latifolium extract as corrosion inhibitor for aluminum alloy in HCl solutions. Journal of Molecular Structure, 1302, 137508. <https://doi.org/10.1016/j.molstruc.2024.137508>
- Wan Nik, W. B., Ravindran, K., Al-Amiery, A. A., Izionworu, V. O., Fayomi, O. S. I., Berdimurodov, E., Daoudi, W., Zulkifli1, F., Dhande, D. Y., 2023. Piper betle extract as an eco-friendly corrosion inhibitor for aluminium alloy in hydrochloric acid media. Int. J. Corros. Scale Inhib., 12(3), 948–960. <http://doi.org/10.17675/2305-6894-2023-12-3-9>